

|                     |   |
|---------------------|---|
| <b>Zeitschrift:</b> | Schweizerische mineralogische und petrographische Mitteilungen =<br>Bulletin suisse de minéralogie et pétrographie          |
| <b>Band:</b>        | 79 (1999)   |
| <b>Heft:</b>        | 3   |
| <b>Artikel:</b>     | The Mont-Mort metapelites : Variscan metamorphism and geodynamic context (Briançonnais basement, Western Alps, Switzerland) |
| <b>Autor:</b>       | Giorgis, David et al.   |
| <b>DOI:</b>         | <a href="https://doi.org/10.5169/seals-60214">https://doi.org/10.5169/seals-60214</a>                                       |

### **Nutzungsbedingungen**

Die ETH-Bibliothek ist die Anbieterin der digitalisierten Zeitschriften auf E-Periodica. Sie besitzt keine Urheberrechte an den Zeitschriften und ist nicht verantwortlich für deren Inhalte. Die Rechte liegen in der Regel bei den Herausgebern beziehungsweise den externen Rechteinhabern. Das Veröffentlichen von Bildern in Print- und Online-Publikationen sowie auf Social Media-Kanälen oder Webseiten ist nur mit vorheriger Genehmigung der Rechteinhaber erlaubt. [Mehr erfahren](#)

### **Conditions d'utilisation**

L'ETH Library est le fournisseur des revues numérisées. Elle ne détient aucun droit d'auteur sur les revues et n'est pas responsable de leur contenu. En règle générale, les droits sont détenus par les éditeurs ou les détenteurs de droits externes. La reproduction d'images dans des publications imprimées ou en ligne ainsi que sur des canaux de médias sociaux ou des sites web n'est autorisée qu'avec l'accord préalable des détenteurs des droits. [En savoir plus](#)

### **Terms of use**

The ETH Library is the provider of the digitised journals. It does not own any copyrights to the journals and is not responsible for their content. The rights usually lie with the publishers or the external rights holders. Publishing images in print and online publications, as well as on social media channels or websites, is only permitted with the prior consent of the rights holders. [Find out more](#)

**Download PDF:** 08.02.2026

**ETH-Bibliothek Zürich, E-Periodica, <https://www.e-periodica.ch>**

# The Mont-Mort metapelites: Variscan metamorphism and geodynamic context (Briançonnais basement, Western Alps, Switzerland)

by David Giorgis<sup>1,2</sup>, Philippe Thélin<sup>1</sup>, Gérard Stampfli<sup>2</sup> and François Bussy<sup>1,3</sup>

## Abstract

The Mont-Mort metapelites are one of the best preserved relics of the Variscan unit in the Briançonnais basement. These micaschists crystallized during a poly-phase metamorphic cycle, under amphibolite facies conditions. Mineral parageneses and geothermobarometric calculations indicate a two-stage evolution. Stage (1) (550–600 °C and 5–8 kbar) is documented by assemblages of zoned garnet, staurolite, kyanite(?), biotite, muscovite, quartz and plagioclase. Stage (2) (550–600 °C and 2 kbar) is illustrated by assemblages of andalusite, sillimanite, muscovite, biotite. This metamorphic evolution is characterized by a nearly isothermal decompression path, terminating with the formation of andalusite-bearing veins.

U–Pb monazite dates at 330 Ma and  $^{40}\text{Ar}/^{39}\text{Ar}$  muscovite dates at 290–310 Ma (without substantial evidence of argon resetting) point to Variscan metamorphism and yield an estimate of the time interval between the thermal peak and the retrogression stage within this part of the Briançonnais basement.

Restoring the Briançonnais and other Alpine basement units within an existing geodynamic model of Cordillera construction and destruction, it is possible to understand better the transition from a medium pressure/high temperature regime (collision with a peak metamorphism around 330 Ma) to low-P/high-T conditions (decompression in an extensional regime) with high geothermal gradient, as recorded by the successive Variscan parageneses within the Mont-Mort metapelites.

**Keywords:** Metapelites, Variscan, Briançonnais basement, U–Pb ages,  $^{40}\text{Ar}/^{39}\text{Ar}$  ages, PalaeoTethys.

## 1. Introduction

The Middle Penninic domain in the Valais (CH), Aosta Valley (It) and in Savoie (Fr) is characterized by an Alpine (Tertiary) metamorphic overprint of middle to upper greenschist facies. Preexisting mineral assemblages are usually severely obliterated, often mylonitized, and pre-Tertiary structural and textural fabrics are generally not preserved. Fortunately, a few areas escaped the Alpine overprint (e.g. lenses of Palaeozoic eclogite, THÉLIN et al., 1990) and still record part of their Palaeozoic history. In the Penninic domain, the Mont-Mort metapelites are probably one of the best examples of very well preserved pre-Mesozoic metamorphic assemblages.

The Mont-Mort metapelites are located near the Grand St. Bernard pass, in the internal Ruitor zone (BURRI, 1983; BAUDIN, 1987; THÉLIN, 1992; DESMONS, 1992; GOUFFON, 1993; GOUFFON and BURRI, 1997) of the Pontis nappe in the western Valais (Briançonnais domain, ESCHER et al., 1993; THÉLIN et al., 1993). On the basis of detailed field work (BURRI, 1983; GIORGIS, 1997), a comprehensive textural, mineralogical and geochronological study of these metapelites was undertaken in order to precisely establish the pre-Alpine P-T-t evolution and to discuss the Palaeozoic geodynamics of the external Briançonnais domain.

<sup>1</sup> Institut de Minéralogie et de Pétrographie, Université de Lausanne, BFSH2, CH-1015, Lausanne, Switzerland.  
[<dgiorgis@imp.unil.ch>](mailto:<dgiorgis@imp.unil.ch>)

<sup>2</sup> Institut de Géologie et de Paléontologie, Université de Lausanne, BFSH2, CH-1015, Lausanne, Switzerland.

<sup>3</sup> Department of Geology, Royal Ontario Museum, Toronto, Canada, M5S 2C6.

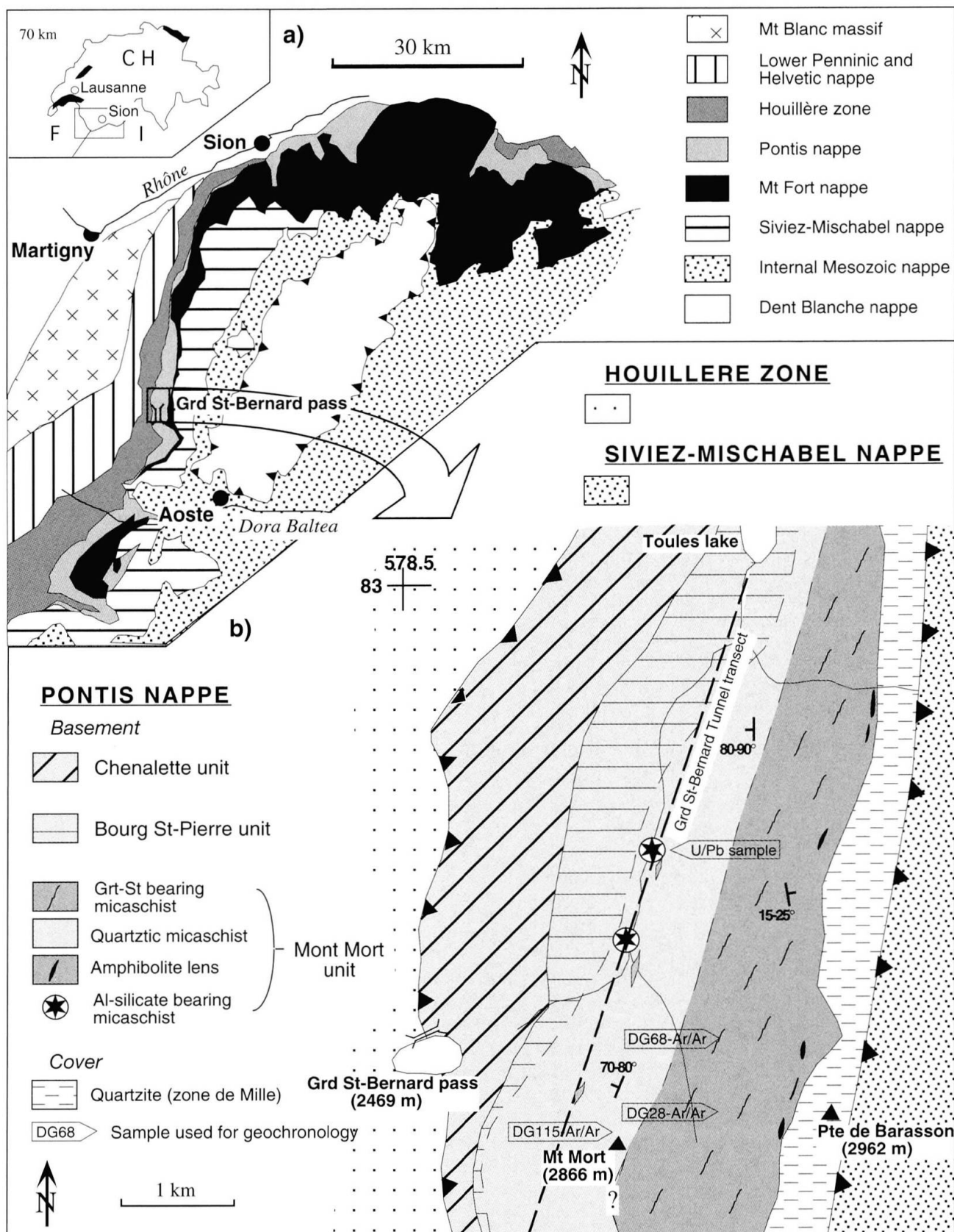


Fig. 1 (a) Tectonic map of the Penninic nappes (modified after GOUFFON, 1993 and THÉLIN et al., 1993). (b) Simplified geological sketch map of the Pontis nappe basement, near the Grand St. Bernard pass area (modified after GOUFFON and BURRI, 1997 and GIORGIS, 1997).

## 2. Geological setting

The Mont-Mort unit belongs to the polygenic Pontis nappe (Fig. 1a) (ESCHER et al., 1993; THÉLIN et al., 1993), which is part of the Grand St. Bernard "super-nappe". It outcrops in the eastern Valais region, as the Berisal complex and the upper Stalden zone, and in the west as the Ruitor zone. The western part of the latter was affected by middle greenschist facies conditions (3–5 kbar, 350–400 °C, GOUFFON, 1993; THÉLIN et al., 1994). In the Grand St. Bernard pass area, the Pontis nappe basement was subdivided by BURRI (1983) and GOUFFON (1993) into three distinct units, from W to E (Fig. 1b): (a) the Chenalette unit, made of fine-grained grey gneisses; (b) the Bourg St. Pierre unit made of orthogneisses and mafic rocks; (c) the Mont-Mort unit made mostly of micaschists.

The Mont-Mort unit is well developed near the Grand St. Bernard pass, where it is limited to the east by quartzites of the Mille zone (Permo-Carboniferous cover of the Pontis nappe) and westward by the Bourg St. Pierre unit. The Mont-Mort unit is mainly composed of a thick metapelitic series, consisting of quartz-rich micaschists overlain by garnet-staurolite micaschists, which occur as two more-or-less parallel N–S trending bands (Fig. 1b). Quartzites, felsic banded gneisses and mafic rocks (amphibolitic gneisses) occur sporadically within the two main lithologies. Special attention was devoted to small and well limited lenses rich in Al-silicates and andalusite-quartz veins (mentioned in Fig. 1b).

The main tectonic features are a well-developed N290–330° schistosity with variable dip (20–90°) and some small Alpine folds, warped towards SE (BURRI, 1983).

## 3. Mineralogy and textures

The Mont-Mort lithologic units have been described repeatedly (OULIANOFF and TRÜMPY, 1958; HEDIGER, 1979; BURRI, 1983; THÉLIN, 1992; GOUFFON, 1993; GOUFFON and BURRI, 1997). In these, metapelites reveal diagnostic mineral parageneses which are considered below. Al-silicate-bearing lenses were first mentioned by OULIANOFF and TRÜMPY (1958), and more precisely located by BURRI (1983) and THÉLIN (1992), e.g. at "the Hospitalet" (Swiss coordinates: 580500/81590) and "the Plan des Dames" (580130/80750). They are more abundant in the western (quartz-rich) than in the eastern (garnet-staurolite) micaschists (Fig. 1b).

The micaschists contain garnet, biotite, white

mica, staurolite, chloritoid, plagioclase (albite and oligoclase), andalusite, sillimanite, chlorite, quartz with minor blue amphibole, stilpnomelane, apatite, monazite, zircon, tourmaline, titanite, ilmenite and rutile (Fig. 2).

Whole-rock geochemistry reflects a typical metapelitic composition with  $\text{Al}_2\text{O}_3$  contents between 18 and 23 wt% (Tab. 1). Al-silicates are not specifically developed in the most Al-rich rocks, which implies that other parameters are involved in the growth and/or preservation of these minerals (THÉLIN, 1992 and GIORGIS, 1997).

### 3.1. PRE-ALPINE EVENTS

The following succession of metamorphic recrystallization events is proposed (Fig. 3) on the basis of textures and microprobe analyses.

#### *Metamorphic event 1a:*

Formation of a now relic schistosity, accompanied by the following phases: garnet-muscovite-biotite-tourmaline-titanite-opaque minerals. This first assemblage is poorly exposed and only survives as inclusions within younger minerals. Garnets are small (0.1–0.5 mm) and sometimes idiomorphic (the so-called "minute garnet"). They are often included within the plagioclase (as in event 1b) and their almandine-rich composition is homogeneous and similar to that of garnets associated with the metamorphic event 1b.

#### *Metamorphic event 1b:*

Crystallization of the second assemblage is characterized by zoned garnet-quartz-plagioclase-muscovite-biotite-staurolite-apatite-(monazite). These minerals include the relic 1a-schistosity as trails of helicitic inclusions, either straight or microfolded. Garnets of the second generation (2–15 mm in diameter) are rich in almandine (72–82 mol. %), with minor amounts of pyrope (7–10%), grossular (5–11%) and spessartine (8–12%). This range of compositions is typical of amphibolite facies pre-Alpine garnets of the Ruitor zone (GOUFFON, 1993). The compositional profiles in the garnets are characterized by core to rim decreases in  $X_{\text{sps}}$  and increases in  $X_{\text{alm}}$  and  $X_{\text{prp}}$  (Fig. 4 and Tab. 1) which suggest growth zoning.

Staurolite (1–10 mm) is often idiomorphic and twinned with inclusions of tourmaline and opaque minerals that form a relic helicitic schistosity. Chemical composition is perfectly homogeneous with 12.7 wt%  $\text{FeO}_{\text{tot}}$ , < 1.5%  $\text{MgO}$ , 0.5%  $\text{ZnO}$  and 0.2%  $\text{MnO}$  (Tab. 1).

Plagioclase forms porphyroblasts with numerous inclusions of opaque minerals, white mica,

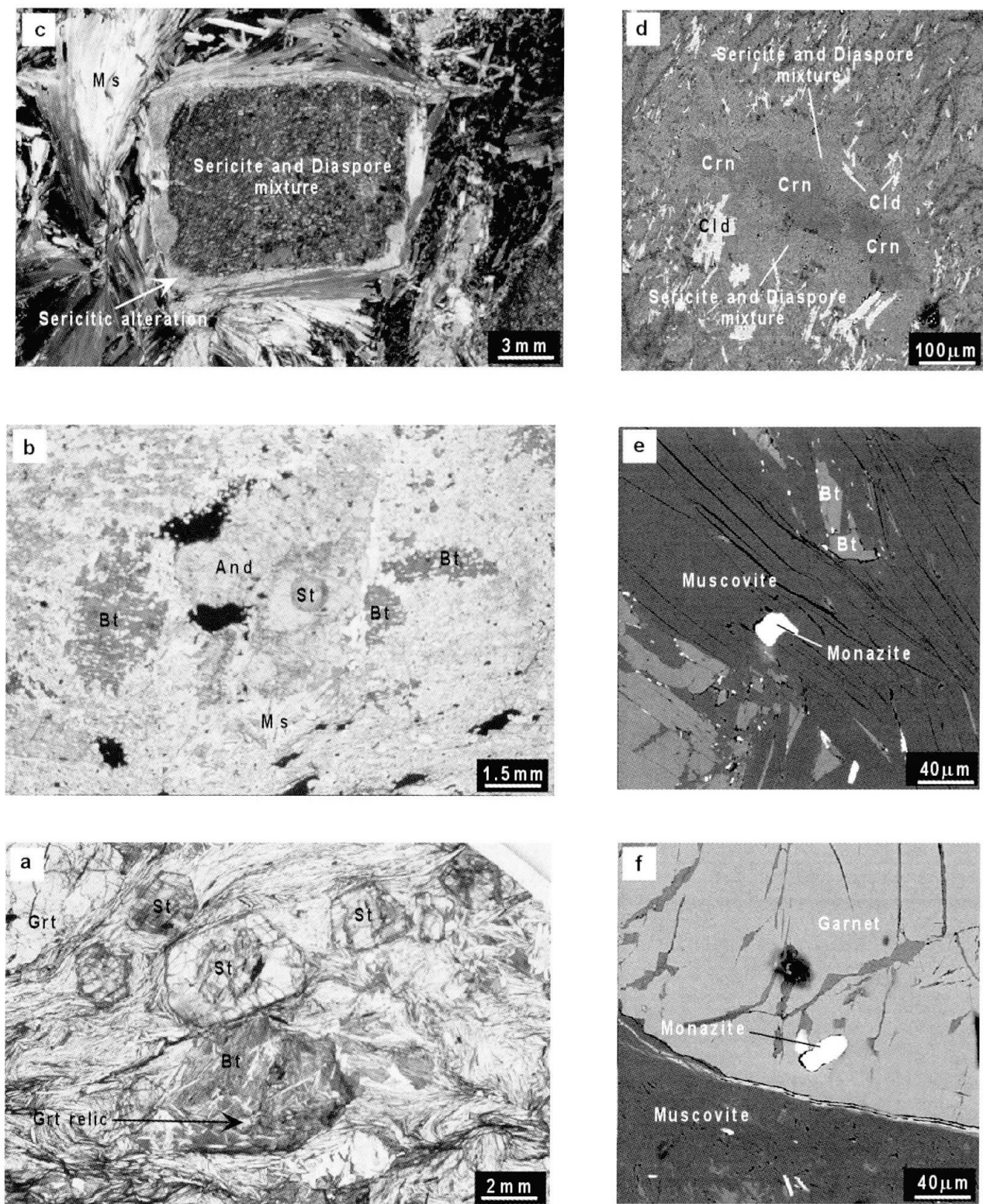


Fig. 2 Petrographic observations. (a) Granolepidoblastic texture, from a Grt-St micaschist, where the main schistosity is well marked and wrapped around staurolite (St). Note the presence of a garnet relic (Grt) strongly retro-morphosed to biotite (Bt). (b) Poikiloblastic andalusite (And) overgrows staurolite (St), showing the clear relation between andalusite appearance and staurolite disappearance in Al-silicate schist. (c) Completely pseudomorphosed andalusite (corundum, chloritoid, sericite and diaspore) within quartz-andalusite vein. (d) BSE photograph of the typical mineral assemblage resulting from andalusite retrogression (in veins). Corundum (Crn) inclusions, considered as relics, are surrounded by chloritoid (Cld) and a mixture of diaspore and sericite. (e) BSE photograph of monazite inclusion in muscovite which define main schistosity ( $s_m$ ). (f) BSE photograph of monazite inclusion in garnet rim. The photos (2e) and (2f) illustrate the textural relationship of monazite in the sample used for U/Pb monazite dating.

|                    | Pre-Alpine metamorphism |            |                            | Alpine metamorphism |                    |
|--------------------|-------------------------|------------|----------------------------|---------------------|--------------------|
|                    | Relic schistosity       |            | Main schistosity ( $s_m$ ) |                     | Alpine schistosity |
| GARNET             | —                       | —          | —                          |                     |                    |
| STAUROLITE         | —                       | —          | —                          |                     |                    |
| MUSCOVITE          | —                       | —          | —                          |                     |                    |
| BIOTITE            | —                       | —          | —                          |                     |                    |
| PLAGIoclASE        | —                       | OLIGOCLASE | —                          | —                   | ALBITE             |
| SILLIMANITE        | —                       | —          | —                          | —                   | —                  |
| ANDALUSITE         | —                       | —          | —                          | —                   | —                  |
| CHLORITOID         | —                       | —          | —                          | —                   | —                  |
| BLUE AMPHIBOLE     | —                       | —          | —                          | —                   | —                  |
| CHLORITE           | —                       | —          | —                          | —                   | —                  |
| APATITE & MONAZITE | —                       | —          | —                          | —                   | —                  |
| ILMENITE           | —                       | —          | —                          | —                   | —                  |
| QUARTZ             | —                       | —          | —                          | —                   | —                  |
| metamorphic events | 1a                      | 1b         | 1c                         | 1d                  | 2a                 |
|                    |                         |            |                            |                     | 2b,c               |

Fig. 3 Summary of observed relations between growth of main mineral phases and microstructures in the northern part of the Mont-Mort unit.

tourmaline, biotite, zircon and minute garnet; the latter defines a relic schistosity. The composition of the preserved crystals is An15–20, but local retrogression shifts values down to pure albite, which suggests that the initial An content of this mineral could have been higher. THÉLIN (1992) reported a weak normal zoning at grain rims.

A second generation of biotite and muscovite grew during the 1b event. Biotite has a composition (22–24 wt%  $FeO_{tot}$ ) similar to that of biotite grown during the subsequent 1c and 1d events.

#### Metamorphic event 1c:

This event is defined by the formation of the main schistosity ( $s_m$ ) and continuous growth of biotite and muscovite that embed pre-existing por-

phyroblasts. Muscovite has a composition similar to that of other generations, with a very low celadonitic substitution ( $Si (IV) < 3.1$  p.f.u.) and low  $Fe_{tot}$  ( $< 0.2$  p.f.u.) and Mg ( $< 0.2$  p.f.u.) contents (Fig. 5 and Tab. 1). Chemical composition of the 1c biotite is homogeneous (Fig. 6 and Tab. 1). It is locally retrogressed into chlorite.

#### Metamorphic event 1d:

Crystallization of a new assemblage of biotite-muscovite-andalusite-sillimanite-quartz defines event 1d. The appearance of these minerals is accompanied by the retrogression of zoned garnet to biotite (see Fig. 2a), retrogression of older biotites to sillimanite (THÉLIN, 1992; BURRI, 1983) and formation of an andalusite-biotite-muscovite

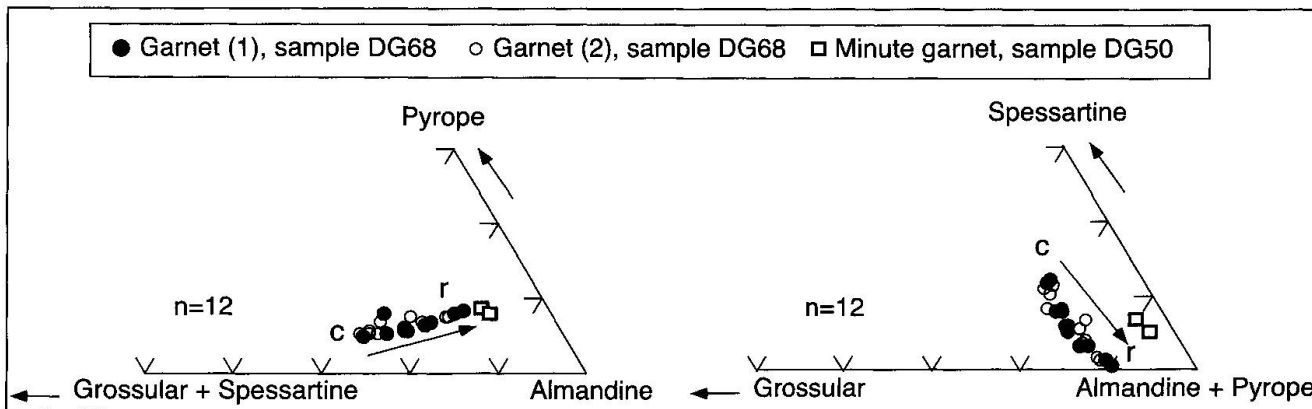


Fig. 4 Chemical zoning in garnet (c = core, r = rim).

**Tab. 1** (a) Representative microprobe analyses of the main minerals within Mont-Mort metapelites. Analytical conditions were 15 kV and a sample current of 20 nA (na = not analyzed). (b) Representative bulk rock composition (by XRF) of the Mont-Mort metapelites (n = 2).

assemblage at the expense of staurolite (Fig. 2b). Andalusite has a poikiloblastic idiomorphic habit, including the main schistosity ( $s_m$ ), and a regular chemical composition with 0.2–0.3 wt%  $Fe_{tot}$  (Tab. 1). Sillimanite is either massive or fibrolitic. The chemical homogeneity across all generations of micas might result from a partial reequilibration (migration or diffusion) during 1d or later (?).

Phengite, cordierite and K-feldspar are not found in these metapelites. The presence of kyanite as noted by OULIANOFF and TRÜMPY (1958) was also not observed. All white micas analyzed with XRD in these rocks are  $2M_1$  polytypes (HEDIGER, 1979; THÉLIN et al., 1994).

The mineral associations described above belong to the amphibolite facies. Because this middle-grade facies was never attained in the Briançonnais domain during the Alpine orogeny (at least within the sector west of the Simplon line), these parageneses and their associated schistosity have always been logically attributed to a pre-Alpine metamorphic event.

### 3.2. ALPINE EVENTS

#### *Metamorphic event 2a:*

Event 2a includes partial retrogression of plagioclase, in the "Na-rich" metapelites, to ferroglaucophane (GIORGIS, 1997) and formation of the latter within the matrix.

#### *Metamorphic event 2b, 2c:*

Growth of the main Alpine schistosity and re-orientation of the pre-Alpine schistosity ( $s_m$ ) defines events 2b and 2c. This leads to the local deformation of some pre-existing minerals (garnet and staurolite), and to partial retrogression of the assemblages. This includes: (a) partial chloritization of ferroglaucophane, garnet and biotite; (b) albitization and partial sericitization of plagioclase; (c) partial sericitization of staurolite and growth of chloritoid after staurolite, and (d) growth of stilpnomelane.

### 3.3. QUARTZ-ANDALUSITE VEINS

The Mont-Mort metapelites contain quartz-andalusite veins 10 cm to 4 m long, composed of grey quartz in a black sericite-rich matrix (originally quartz, andalusite and white mica, with occasional plagioclase). These veins are strongly deformed and boudinaged along the Alpine schistosity, but some of them cut the latter at a low angle (15–20°).

Quartz is bulky, with a grey color and a dark aspect. Andalusite is completely pseudomorphed by various minerals, such as corundum (microprobe identification, Photo 2d), diaspore (XRD identification), chloritoid and sericite. These ghost crystals sometimes show a typical prismatic euhedral habit (up to 10 cm long and 2 cm in cross-section)

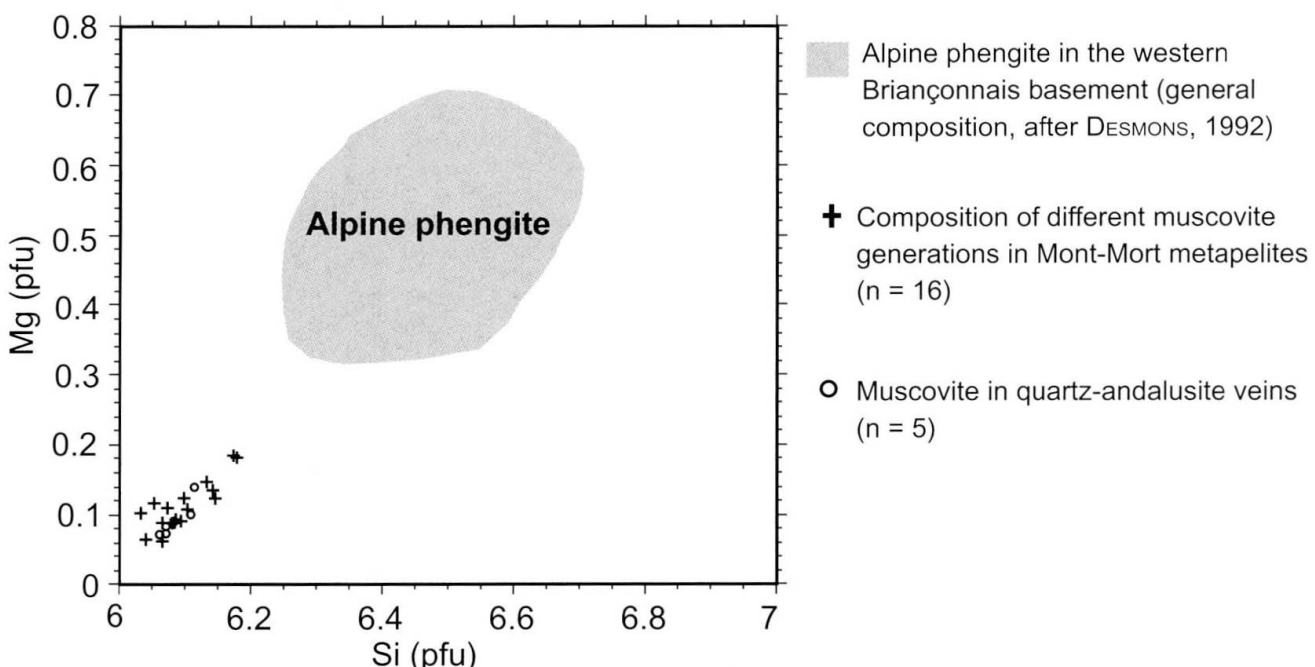


Fig. 5 Si–Mg diagram showing the homogeneous composition of different textural generations of muscovite. Note the low content in Si and Mg, compared to the general composition of Alpine phengites occurring within the western Briançonnais basement (DESMONS, 1992). (p.f.u. = per formula unit).

(Fig. 2c), and a black color due to alteration. Different generations of white mica can be identified, that are 2M<sub>1</sub> polytypes. There is an early generation of coarse primary muscovite (1 cm) with a chemical composition identical to that of the various generations of muscovite observed within the metapelites (Fig. 5 and Tab. 1). Subsequent generations consist of muscovite (finely crystallized from andalusite) and sericite. The sericite consists of an intergrowth of muscovite and paragonite. Feldspar is rare but where present, XRD analysis suggests an albite composition.

Structural evidence indicates that these veins pre-date Alpine deformation but post-date Variscan structures. The incompatibility between the andalusite crystallization and the Alpine greenschist metamorphic conditions known in the area (GOUFFON, 1993), point to a late-Variscan metamorphic origin.

#### 4. Metamorphism and P-T path

P-T conditions were estimated using published mineral stability curves for metapelites in the KMASH system (K<sub>2</sub>O–FeO–MgO–Al<sub>2</sub>O<sub>3</sub>–SiO<sub>2</sub>–H<sub>2</sub>O) (SPEAR and CHENEY, 1989), as well as theoretical data from YARDLEY (1989) and HOSCHEK (1969) on mineral reactions. They were further constrained by cation-exchange geothermometers.

#### 4.1. MINERAL STABILITY CURVES

Crystallization-deformation textural relationships record two successive mineral assemblages. The first one, composed of Grt-St-Bt-Ms-Pl (1b metamorphic event), is stable in a rather wide P-T range (SPEAR, 1993). Nevertheless, the high almandine content and the classical zoning of the garnet (SPEAR, 1993), as well as the appearance of the Bt-St pair related to the reaction Grt + Ch + Ms = St + Bt + H<sub>2</sub>O (curve 1, Fig. 7), imply a minimal temperature of 550–600 °C. The local presence of kyanite (OULIANOFF and TRÜMPY, 1958 and SILVANA MARTIN, pers. com., 1998) further constrains the system to slightly higher conditions beyond the stability curve of reaction (2) St + Chl = Bt + As and above the Ky-Sill boundary, in field (b) of figure 7. P-T conditions would thus have been higher than 600 °C and 6 kbar. These values are consistent with P estimates > 5 kbar using the GMAP geothermobarometer of GHENT and STOUT (1981). Kyanite has also been reported by BOCQUET [DESMONS] (1974) in the southern part of the Ruitor zone. According to BAUDIN (1987), this mineral was, as in the Mont-Mort area, an early phase, that belonged to the garnet-staurolite assemblage and predated the main regional schistosity.

Sillimanite crystallized after the Grt-St-Bt-Ms-Pl assemblage, which documents the early

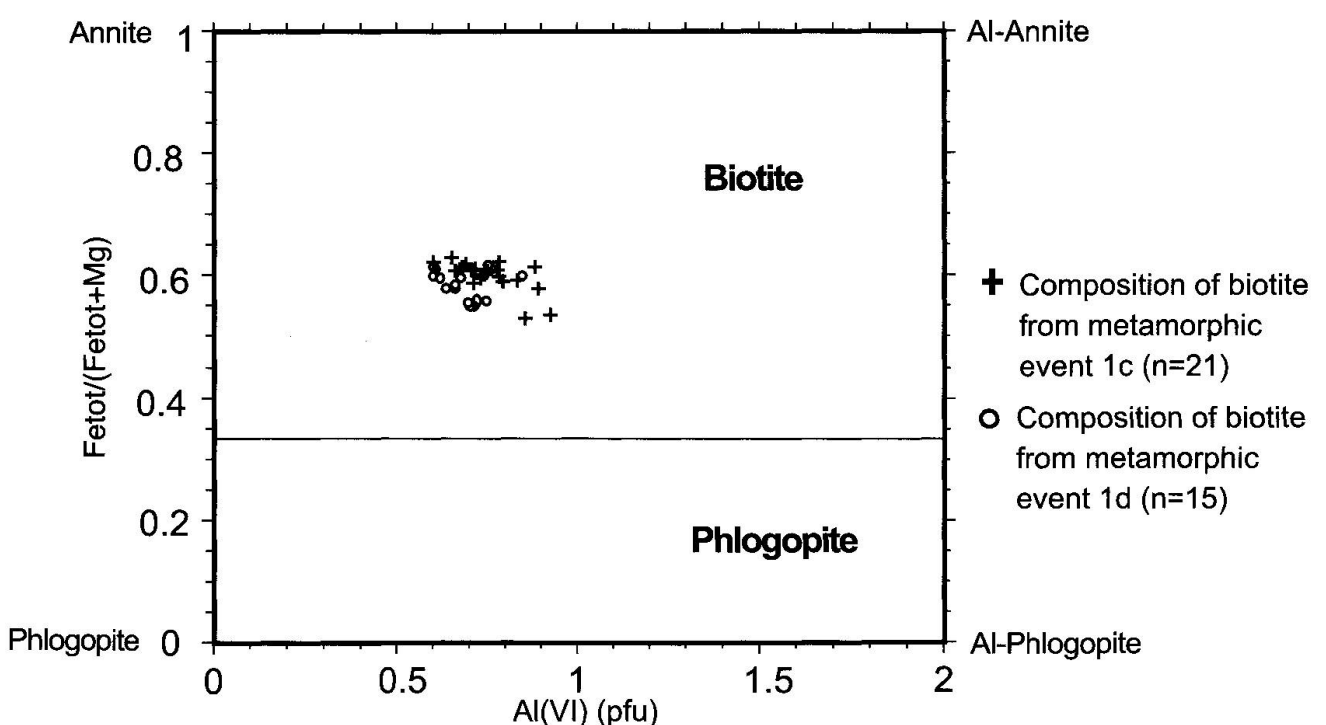


Fig. 6 GUIDOTTI (1984) classification diagram, showing no major chemical difference between the texturally different types of biotite in Mont-Mort metapelites.

stage of isothermal decompression. The second assemblage is characterized by the appearance of andalusite, new generations of muscovite and biotite (metamorphic event 1d). These minerals grew at the expense of staurolite. The disappearance of staurolite might be related to the reactions (3)  $St = Alm + As + H_2O$  and (4)  $St + Ms + Qtz = And + Bt + H_2O$  (Fig. 7) from SPEAR (1993) and HOSCHEK (1969), respectively. On the other hand, the absence of K-feldspar implies that reaction (5)  $Ms + Qtz = Kfs + As + H_2O$  (SPEAR, 1993) did not occur. Consequently, the metamorphic assemblage 1d is confined in field c of figure 7 (i.e. at conditions around 550–600 °C and 1–2 kbar).

#### 4.2. GEOTHERMOMETRY

The garnet-biotite geothermometer was used to estimate the temperature of the metamorphic

event 1b defined by the assemblage Grt-St-Bt-Ms-Pl. Microprobe analyses were performed on either side of Grt-Bt grain boundaries on biotite crystals defining the main schistosity. Temperatures were calculated using experimental calibrations of HODGES and SPEAR (1982), assuming an ideal ionic solution for garnet, a correction for its Ca content, a pressure of 3 kbar, and considering the total Fe content of biotite. Results are in the range of 550–600 °C. The interpretation of this result is difficult. However assuming the relative high re-equilibration capacity of the Fe–Mg exchange between garnet and biotite using rim thermometry (VANNAY and GRASEMANN, 1998), we think that it is more realistic to interpret this result as a re-equilibration temperature that was set during or after the metamorphic event 1d (c field in Fig. 7).

The garnet-staurolite Fe/Mg cation-exchange thermometer of PERCHUK (1991) was also applied

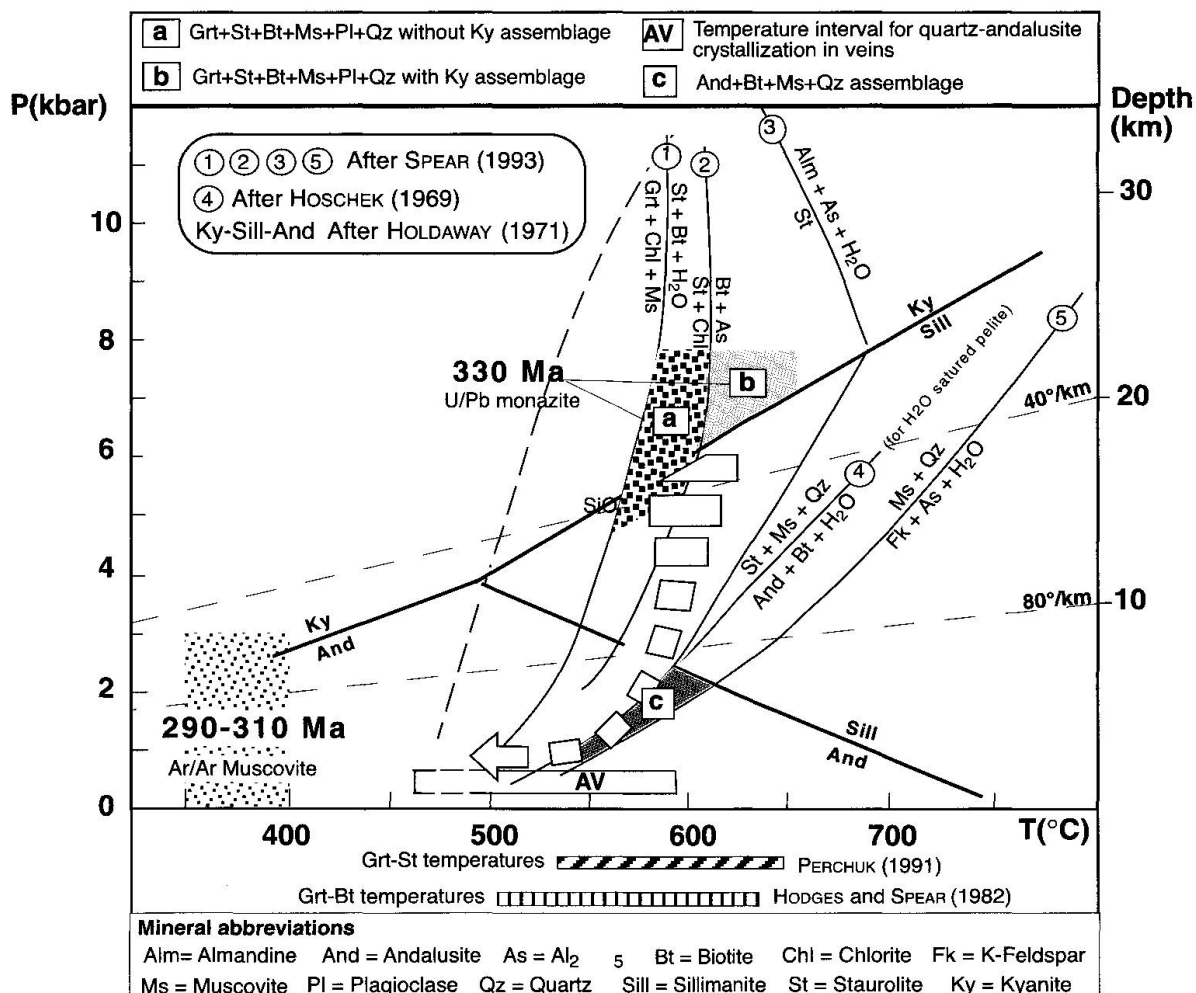


Fig. 7 P-T-t path of the pre-Alpine metamorphic evolution of the Mont-Mort unit. The late-Variscan metamorphic evolution (particularly for the alteration of the quartz-andalusite veins) still remains uncertain. Reactions from SPEAR (1993) correspond to reactions in the KFMASH system. Cross-hatched thick lines at the bottom of the diagram represent the range of estimates obtained by cation exchange thermometry. U/Pb geochronological data for metamorphic peak are from BUSSY et al. (1996a) and the  $^{40}Ar/^{39}Ar$  cooling age below 400 °C are from this work.

to calculate crystallization temperatures of the Grt-St-Bt-Ms-Pl assemblage, using garnet core compositions and assuming a pressure of 5 kbar. The average temperature obtained is approximately 600 °C, which is compatible with the previously established position of fields a and b in figure 7. This value is in agreement with results obtained by DESMONS (1992) on a Grt-St-Bt mineral assemblage in the southern part of the Ruitor zone. The absence of chemical zoning in staurolite might be interpreted as a re-equilibration feature related to the late high-T/low-P event at the time of equilibration for the And-Ms-Bt-Qtz assemblage. But considering the differential growth kinetics between staurolite and garnet, as well as the low diffusion rates of Fe and Mg in staurolite (SPEAR, 1993), the staurolite chemical homogeneity is instead interpreted as original, and the calculated temperatures are considered to be those prevailing at time of the crystallization of the Grt-St-Ms-Bt-Pl assemblage.

#### 4.3. P-T PATH EVOLUTION

Although poorly constrained in terms of pressure, the P-T path obtained shows an evolution within the amphibolite facies with a strong isothermal decompression towards low pressure parageneses (Fig. 7). This high-grade metamorphic evolution is totally incompatible with the regional Alpine conditions and is thus interpreted as pre-Alpine.

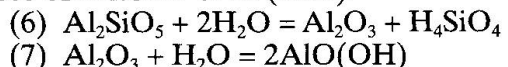
As far as the Alpine metamorphism is concerned, the Ruitor zone reveals a typical greenschist facies assemblage with chlorite, chloritoid, ferroglaucophane, albite, sericite, and P-T conditions around 5 kbar and 350–400 °C (GOUFFON, 1993). On the other hand, this Alpine assemblage is weakly developed within the Mont-Mort unit and seems to correspond to P-T conditions lower than in the rest of the Ruitor zone. The reason (likely structural or chemical ?) for the less intense Alpine overprint in the Mont-Mort area is not yet understood.

#### 4.4. QUARTZ-ANDALUSITE VEINS AND THEIR SIGNIFICANCE IN THE METAMORPHIC EVOLUTION

The andalusite-bearing veins are pre-Alpine for the reasons developed above and most probably result from the circulation of Al-rich fluid. According to BRUGGER (1994), such fluid might result from the dehydration of staurolite (reaction 4, Fig. 7). This would imply a synchronous crystallization of andalusite in metapelites and in veins,

which is consistent with textural observations, but other reactions cannot be ruled out.

The subsequent alteration of andalusite to corundum, diaspore and sericite might potentially be related either to a late pre-Alpine retrogression or to the Alpine greenschist facies metamorphism. Crystallization of corundum has often been reported, although in unspecified metamorphic conditions (e.g. ROSE, 1957; MASON, 1978; SHULTERS and BOHLEN, 1989). The only published reactions compatible with the Mont-Mort mineral assemblage and metamorphic conditions are those of HEMLEY et al. (1980):



According to these authors, reaction (6) occurs between 400–500 °C ( $P_{\text{H}_2\text{O}} \sim 1\text{--}1.5$  kbar), also depending slightly on the  $\text{SiO}_2$  concentration in the fluids. These conditions are not compatible with the Alpine greenschist facies metamorphism, and we must consider that the hydrothermal alteration of andalusite to corundum occurred during the retrograde pre-Alpine metamorphic path. This conclusion is based on the assumption that corundum is indeed a product of andalusite alteration, rather than coeval with – or older than – the andalusite crystallization, as postulated by SPAENHAUER (1933) for andalusite-corundum-bearing veins of the Silvretta nappe (Central Alps).

Crystallization of diaspore through reaction (7) occurs at around 400 °C and  $P_{\text{H}_2\text{O}} = \sim 1\text{--}1.5$  kbar, depending slightly on the  $\text{SiO}_2$  content of the fluid. Such low-grade conditions have been reached both during late pre-Alpine evolution and Alpine greenschist facies metamorphism. Consequently, the appearance of diaspore cannot be safely linked to one or the other of the two events. The same is true for other low-grade alteration minerals, such as chloritoid and sericite, whose very small size did not allow temperature estimates (paragonite-muscovite geothermometer).

In conclusion, andalusite-bearing veins could reflect a high geothermal gradient in the Mont-Mort unit. But several fundamental questions remain open, such as the exact source of the Al-rich fluids and the nature and timing of the veining process: was it synmetamorphic or not? Did andalusite grow simultaneously in veins and host rocks? Was it a hydrofracturing process? Did veins form by simple diffusion or by fluid flow from the surrounding rocks? The almost complete retrogression of the veins into low-grade mineral assemblages makes it difficult to solve these questions.

## 5. Geochronological constraints

Chronological data available for the Grand St. Bernard nappe, particularly the western Briançonnais basement, have been very scarce (BOCQUET [DESMONS] et al., 1974; SOOM, 1990; HUNZIKER et al., 1992). Thus, new isotopic analyses were performed in order to better constrain the timing of the exceptionally well-preserved pre-Alpine metamorphism of the Mont-Mort area.

### 5.1. U/Pb MONAZITE DATA

U/Pb dating of two multigrain monazite fractions from the Mont-Mort metapelites was recently carried out by BUSSY et al. (1996a), using conventional isotope dilution techniques. Petrographic observations show that most monazite crystals (30–50  $\mu\text{m}$ ) occur as inclusions within muscovite (which marks the main schistosity), or as inclusions within garnet rims (Figs 2e and 2f). So far, no

reaction seems to adequately explain monazite crystallization during metamorphism. However, textural observations are consistent with monazite growth coeval with the Grt-St-Pl-Bt-Ms assemblage.

### 5.2. $^{40}\text{Ar}/^{39}\text{Ar}$ MUSCOVITE DATA

Unlike most metamorphic rocks of the Penninic basement, no white micas (such as phengite) appear to have crystallized in the Mont-Mort metapelites during Alpine greenschist metamorphism. This prompted us to try  $^{40}\text{Ar}/^{39}\text{Ar}$  dating on muscovite, as no mixing phenomena between pre-Alpine muscovites and Alpine phengites were expected to occur. Three muscovite samples (size: 180–250  $\mu\text{m}$ ) were selected and analyzed by conventional  $^{40}\text{Ar}/^{39}\text{Ar}$  step heating methods (for details about the analytical techniques, see COSCA et al., 1998). Biotite, which is often associated with chlorite, was not analyzed.

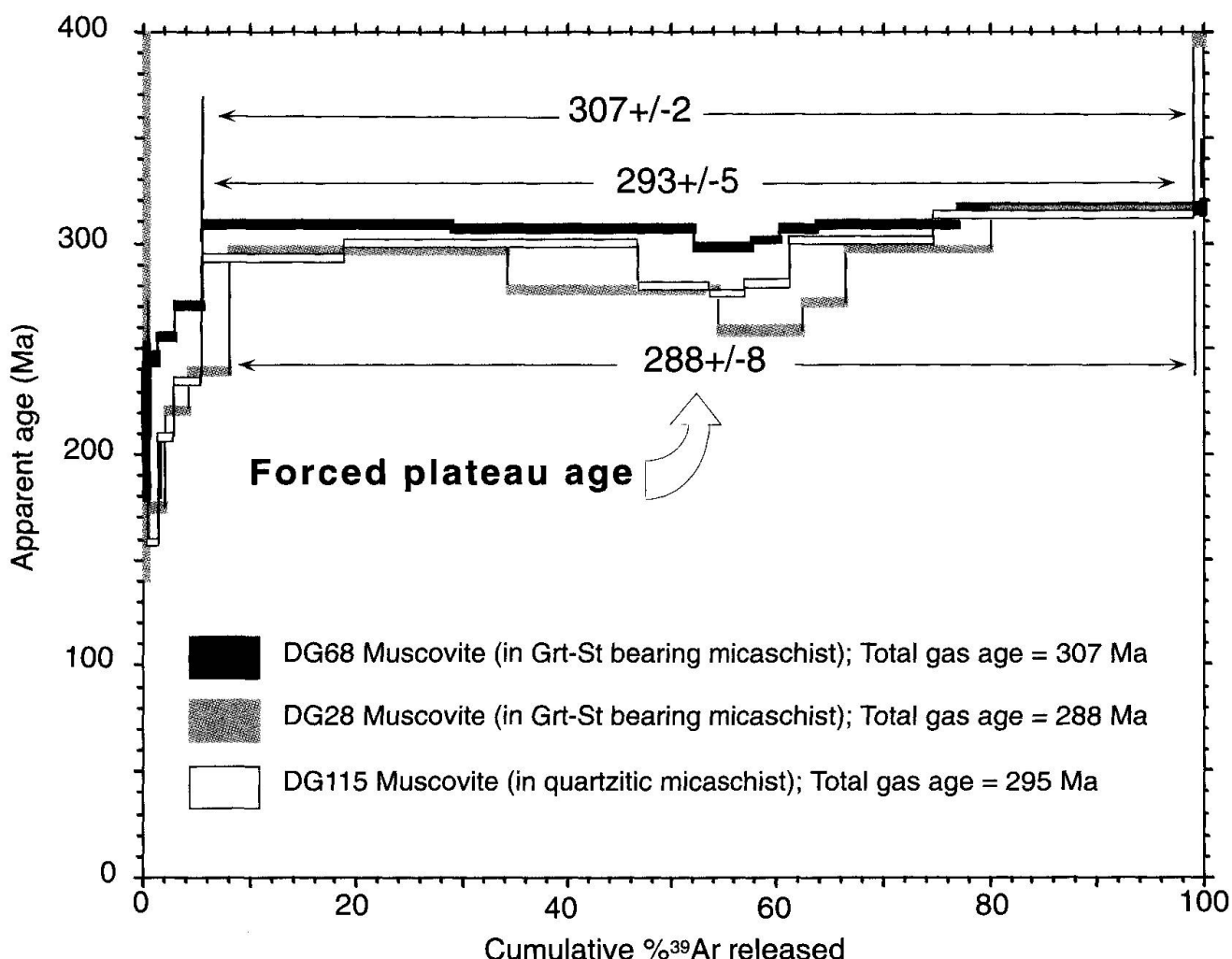


Fig. 8 Age spectrum of pre-Alpine muscovite within the Mont-Mort metapelites.

Tab. 2  $^{40}\text{Ar}/^{39}\text{Ar}$  experimental data for the Mont-Mort muscovites. All data in moles indicate values above baselines corrected only for blank decay and mass discrimination.

| DG68                                 |                              |                              |                              |   |                                  |                      |                        |
|--------------------------------------|------------------------------|------------------------------|------------------------------|---|----------------------------------|----------------------|------------------------|
| T (°C)                               | $^{40}\text{Ar}$<br>x 10E-14 | $^{39}\text{Ar}$<br>x 10E-16 | $^{37}\text{Ar}$<br>x 10E-18 | $^{36}\text{Ar}$<br>x 10E-18  | $^{39}\text{Ar}$<br>(% of total) | % $^{40}\text{Ar}^*$ | Age $\pm 2\sigma$ (Ma) |
| 700                                  | 1350 $\pm$ 4                 | 1394 $\pm$ 3                 | 1129 $\pm$ 44                | 39104 $\pm$ 60  | 0.7                              | 14.4                 | 225.4 $\pm$ 8.7        |
| 800                                  | 274 $\pm$ 2                  | 1643 $\pm$ 10                | 487 $\pm$ 29                 | 777 $\pm$ 8   | 0.9                              | 91.6                 | 245.5 $\pm$ 1.4        |
| 850                                  | 472 $\pm$ 1                  | 2822 $\pm$ 11                | 227 $\pm$ 22                 | 731 $\pm$ 8   | 1.5                              | 95.4                 | 255.8 $\pm$ 0.9        |
| 900                                  | 931 $\pm$ 3                  | 5298 $\pm$ 14                | 236 $\pm$ 27                 | 1128 $\pm$ 9  | 2.8                              | 96.4                 | 270.4 $\pm$ 0.9        |
| 950                                  | 8820 $\pm$ 19                | 44126 $\pm$ 80               | 2643 $\pm$ 224               | 6001 $\pm$ 19   | 23.3                             | 98                   | 309.2 $\pm$ 0.8        |
| 1000                                 | 8560 $\pm$ 13                | 43649 $\pm$ 72               | 3.3 $\pm$ 4.2                | 2531 $\pm$ 12   | 23.0                             | 99.1                 | 307.1 $\pm$ 0.7        |
| 1025                                 | 2070 $\pm$ 4                 | 10856 $\pm$ 26               | 692 $\pm$ 64                 | 828 $\pm$ 9   | 5.7                              | 98.8                 | 298.4 $\pm$ 0.8        |
| 1050                                 | 969 $\pm$ 2                  | 5008 $\pm$ 7                 | 357 $\pm$ 46                 | 500 $\pm$ 7   | 2.6                              | 98.5                 | 301.4 $\pm$ 0.7        |
| 1100                                 | 1240 $\pm$ 3                 | 6279 $\pm$ 14                | 372 $\pm$ 27                 | 653 $\pm$ 7   | 3.3                              | 98.4                 | 307.1 $\pm$ 0.8        |
| 1200                                 | 5040 $\pm$ 7                 | 25471 $\pm$ 52               | 0.2 $\pm$ 2.6                | 2121 $\pm$ 12   | 13.4                             | 98.8                 | 308.5 $\pm$ 0.7        |
| 1400                                 | 8650 $\pm$ 12                | 42734 $\pm$ 54               | 1350 $\pm$ 159               | 1606 $\pm$ 13   | 22.5                             | 99.4                 | 317.1 $\pm$ 0.7        |
| 1650                                 | 105 $\pm$ 1                  | 416 $\pm$ 2                  | 322 $\pm$ 30                 | 720 $\pm$ 9   | 0.2                              | 79.8                 | 316.9 $\pm$ 1.7        |
| weight = 7.77 mg; J value = 0.00955  |                              |                              |                              | Forced plateau age (950–1400 °C) = 307 $\pm$ 2 (Ma)<br>Total gas age = 306.7 $\pm$ 0.3 (Ma) |                                  |                      |                        |
| DG115                                |                              |                              |                              |   |                                  |                      |                        |
| 700                                  | 1940 $\pm$ 9                 | 1100 $\pm$ 6                 | 1397 $\pm$ 118               | 60673 $\pm$ 87  | 0.5                              | 7.6                  | 216.6 $\pm$ 18.5       |
| 800                                  | 273 $\pm$ 1                  | 2199 $\pm$ 4                 | 1549 $\pm$ 40                | 2032 $\pm$ 10   | 0.9                              | 78                   | 159.4 $\pm$ 0.6        |
| 850                                  | 481 $\pm$ 1                  | 3517 $\pm$ 9                 | 552 $\pm$ 30                 | 949 $\pm$ 8   | 1.5                              | 94.2                 | 209.1 $\pm$ 0.6        |
| 900                                  | 983 $\pm$ 2                  | 6432 $\pm$ 17                | 210 $\pm$ 38                 | 1582 $\pm$ 11   | 2.7                              | 95.2                 | 234.6 $\pm$ 0.7        |
| 950                                  | 5990 $\pm$ 9                 | 31483 $\pm$ 60               | 847 $\pm$ 172                | 5824 $\pm$ 17   | 13.2                             | 97.1                 | 293.1 $\pm$ 0.7        |
| 1000                                 | 12800 $\pm$ 42               | 66884 $\pm$ 130              | 480 $\pm$ 111                | 4728 $\pm$ 18   | 28.1                             | 98.9                 | 299.6 $\pm$ 0.8        |
| 1025                                 | 2830 $\pm$ 9                 | 15874 $\pm$ 46               | 371 $\pm$ 47                 | 1152 $\pm$ 9  | 6.7                              | 98.8                 | 280.3 $\pm$ 0.9        |
| 1050                                 | 1450 $\pm$ 5                 | 8218 $\pm$ 15                | 298 $\pm$ 51                 | 904 $\pm$ 9   | 3.5                              | 98.2                 | 276.0 $\pm$ 0.8        |
| 1100                                 | 1800 $\pm$ 4                 | 9996 $\pm$ 16                | 1010 $\pm$ 57                | 1199 $\pm$ 9  | 4.2                              | 98                   | 280.9 $\pm$ 0.7        |
| 1200                                 | 6210 $\pm$ 8                 | 32062 $\pm$ 41               | 3719 $\pm$ 166               | 2904 $\pm$ 16   | 13.5                             | 98.6                 | 302.2 $\pm$ 0.7        |
| 1400                                 | 11500 $\pm$ 14               | 57504 $\pm$ 52               | 2197 $\pm$ 303               | 2340 $\pm$ 16   | 24.2                             | 99.4                 | 313.4 $\pm$ 0.7        |
| 1650                                 | 547 $\pm$ 3                  | 2426 $\pm$ 11                | 412 $\pm$ 24                 | 2011 $\pm$ 13   | 1.0                              | 89.1                 | 316.6 $\pm$ 1.3        |
| weight = 9.74 mg; J value = 0.00955  |                              |                              |                              | Forced plateau age (950–1400 °C) = 293 $\pm$ 5 (Ma)<br>Total gas age = 295 $\pm$ 0.3 (Ma)   |                                  |                      |                        |
| DG28                                 |                              |                              |                              |   |                                  |                      |                        |
| 700                                  | 4630 $\pm$ 11                | 1154 $\pm$ 8                 | 1685 $\pm$ 172               | 149998 $\pm$ 243  | 0.6                              | 4.3                  | 272.9 $\pm$ 65.8       |
| 800                                  | 504 $\pm$ 2                  | 2969 $\pm$ 10                | 1164 $\pm$ 52                | 6324 $\pm$ 22   | 1.6                              | 63                   | 175.2 $\pm$ 1.1        |
| 850                                  | 588 $\pm$ 2                  | 3962 $\pm$ 11                | 602 $\pm$ 30                 | 1541 $\pm$ 10   | 2.1                              | 92.2                 | 221.5 $\pm$ 0.8        |
| 900                                  | 1140 $\pm$ 3                 | 7340 $\pm$ 18                | 602 $\pm$ 46                 | 1629 $\pm$ 9  | 3.9                              | 95.8                 | 239.5 $\pm$ 0.7        |
| 950                                  | 9130 $\pm$ 22                | 47711 $\pm$ 70               | 854 $\pm$ 117                | 6011 $\pm$ 18   | 25.6                             | 98.1                 | 297.2 $\pm$ 0.7        |
| 1000                                 | 6800 $\pm$ 30                | 38579 $\pm$ 127              | 10.3 $\pm$ 4.9               | 1851 $\pm$ 12   | 20.7                             | 99.2                 | 278.4 $\pm$ 0.8        |
| 1025                                 | 1510 $\pm$ 7                 | 9222 $\pm$ 43                | 1217 $\pm$ 68                | 641 $\pm$ 8   | 4.9                              | 98.7                 | 258.9 $\pm$ 1.1        |
| 1050                                 | 1010 $\pm$ 4                 | 6137 $\pm$ 13                | 651 $\pm$ 32                 | 570 $\pm$ 7   | 3.3                              | 98.3                 | 259.1 $\pm$ 0.8        |
| 1100                                 | 1310 $\pm$ 6                 | 7548 $\pm$ 25                | 1676 $\pm$ 64                | 714 $\pm$ 8   | 4.0                              | 98.4                 | 272.4 $\pm$ 0.9        |
| 1200                                 | 4770 $\pm$ 9                 | 25084 $\pm$ 29               | 5945 $\pm$ 165               | 1974 $\pm$ 11   | 13.4                             | 98.8                 | 297.5 $\pm$ 0.7        |
| 1400                                 | 7050 $\pm$ 10                | 34972 $\pm$ 44               | 29097 $\pm$ 510              | 1440 $\pm$ 10   | 18.7                             | 99.4                 | 315.8 $\pm$ 0.7        |
| 1650                                 | 515 $\pm$ 2                  | 1910 $\pm$ 8                 | 1234 $\pm$ 41                | 775 $\pm$ 8   | 1.0                              | 95.5                 | 396.6 $\pm$ 1.4        |
| weight = 10.58 mg; J value = 0.00955 |                              |                              |                              | Forced plateau age (950–1400 °C) = 288 $\pm$ 8 (Ma)<br>Total gas age = 288.1 $\pm$ 0.4 (Ma) |                                  |                      |                        |

### 5.3. RESULTS AND INTERPRETATIONS

The two dated monazite fractions yielded identical concordant U–Pb ages of 330  $\pm$  2 Ma (BUSSY et al., 1996a). The good reproducibility and concor-

dance of the data let us consider this age to be geologically significant (without any apparent inheritance). Considering (1) that the closure temperature of the U/Pb isotopic system for monazite is about 700 °C (MEZGER et al., 1992), which is high-

er than the metamorphic conditions experienced in the Mont-Mort unit, (2) that the metapelites did not experience strong post-crystallization shearing, which might potentially reset the U-Pb isotopic system of monazite, and (3) the above-mentioned textural relationships,  $330 \pm 2$  Ma is interpreted as the age of the Grt-St-B-Ms-Pl peak-metamorphic mineral assemblage (1b event).

The three muscovite samples yielded similar results and gas-release behaviour during step heating (Fig. 8 and Tab. 2). Most of the  $^{39}\text{Ar}$  ( $> 90\%$ ) was degassed during seven of the eleven heating steps, between 950 and 1400 °C. The data did not allow a strict calculation of an age plateau, but the total gas ages obtained (Fig. 8) are between 288 to 307 Ma for all three samples. Unfortunately, the data are tightly clustered when plotted on an isochron diagram, precluding an independent check on the isotope composition of the nonradiogenic argon. Furthermore, we cannot exclude an eventual intra-granular argon remobilization or loss produced by late-Variscan or Alpine deformation, as shown by KRAMAR et al. (in prep.) for the Siviez-Mischabel basement. However, the possibility of having mixed ages is ruled out by the absence of Alpine phengite in these rocks. Finally, despite the uncertainties discussed above and considering the relative short period of time between U/Pb monazite ages (330 Ma) and  $^{40}\text{Ar}/^{39}\text{Ar}$  muscovite ages (290–310 Ma), we interpret the latter age as a metamorphic cooling age. Since the estimated closure temperature for the analyzed size fraction is at least 400 °C (KIRSCHNER et al., 1996), we conclude that the Alpine metamorphic conditions were not high enough to reset the argon isotopic system of these pre-Alpine muscovites, a phenomenon also reported by other authors in the Briançonnais basement. MONIÉ (1990) found Variscan plateau ages (340–360 Ma) on muscovites in the Ambin massif and more recently MARKLEY et al. (1998) also obtained Variscan ages (280–340 Ma) for white micas in the more eastern Briançonnais basement (Siviez-Mischabel nappe).

These various geochronological data are coherent and make it possible to consider the pre-Alpine metamorphism of the Mont-Mort unit as part of the Variscan orogenesis. The  $^{40}\text{Ar}/^{39}\text{Ar}$  ages confirm the U/Pb dating on monazite carried out by BUSSY et al. (1996a) and constrain the duration of the Variscan metamorphism in this part of the Briançonnais basement. The age of the metamorphic peak (as far as pressure is concerned) is estimated at 330 Ma and the passage below ca. 400 °C, during cooling, at 290–310 Ma (Fig. 7).

## 6. The Briançonnais basement during Variscan times

The Palaeozoic geodynamic reconstructions of the Briançonnais domain are very scarce. This is probably due to a lack of geochronological data for pre-Alpine events. Despite this gap, we will discuss the role of the Briançonnais in a Palaeozoic geodynamic model developed by STAMPFLI et al. (in press) for the entire Variscan Cordillera.

### 6.1. SOME ADDITIONAL DATA

The Mont-Mort unit, the Sapey gneiss unit (equivalent of the Pontis nappe after GOUFFON, 1993) studied by DÉTRAZ and LOUBAT (1984) and recently investigated by BERTRAND et al. (1998), the Stalden zone (BEARTH, 1978) and the Gruf unit (structural equivalent of the Mont-Mort unit, located in the Swiss Eastern Penninic Alps, after HUBER, 1999), are all pieces of Briançonnais basement located in the external units and containing pre-Alpine amphibolite facies assemblages. In addition, the U/Pb zircon age of  $323 \pm 7$  Ma of the Costa Citrin intrusion located in the zone Houillère (BERTRAND et al., 1998) taken together with the U/Pb data of this study, are consistent with a late or post-metamorphic intrusion. This intrusion may have occurred during or at the end of the decompression phase recorded in the Mont-Mort metapelites.

In the internal part of the Briançonnais basement, evidence of Variscan events seem to be more discrete. MARKLEY et al. (1998) obtained a Variscan age on micas from the Siviez-Mischabel nappe and the basement of this nappe contains eclogite with presumed eo-Variscan ages. However, no well preserved Variscan parageneses have been described in this more internal part and alkaline Cambro-Ordovician intrusions (500 and 507 Ma) of the Thyon metagranite (BUSSY et al., 1996b) and of the Mont Pourri granophyre (GUILLOT et al., 1991 and 1993) reveal no Variscan overprint. In contrast, late-Variscan magmatic events are frequent in the Penninic basement (Pontis, Siviez-Mischabel, Mt Fort). These include the sub-alkaline Randa orthogneiss (269 Ma, BUSSY et al., 1996a), the Grand-Laget rhyolite (267–282 Ma, BUSSY et al., 1996a), the Turtmannal gabbros (THÉLIN et al., 1993; SARTORI, 1989), the granodioritic Mt Flassin and Vedun intrusions (GOUFFON and BURRI, 1997), and the metabasalts from the Métailler unit (THÉLIN et al., 1993; CHESSEX, 1995).

We note strong similarities between the outer Briançonnais basement and the Helvetic base-

ment (Aiguilles-Rouges and Mont-Blanc crystalline massifs), such as a high geothermal gradient, similar metamorphic P-T paths with decompression and cooling (VON RAUMER, 1983) and geochronological constraints with 327 Ma for the metamorphic peak (BUSSY and HERNANDEZ, 1997). Furthermore, the presence of other very important markers such as Ordovician calc-alkaline granitoids (BUSSY and VON RAUMER, 1993; Thélin and Bussy, in prep.), and eo-Variscan eclogites (LIÉGEOIS and DUCHESNE, 1981; THÉLIN et al., 1990; EISELE et al., 1997) in both basements reinforces the comparison.

## 6.2. SIGNIFICANCE OF BRIANÇONNAIS PRE-ALPINE EVENTS IN PALAEOZOIC GEODYNAMICS

According to STAMPFLI et al. (in press), the Variscan orogenesis results from the collision between the so-called Hun superterrane and Baltica-Avalonia. In this model, the Hun superterrane represents a ribbon-like continent located on the border of Gondwana. Its drifting away from Gondwana corresponds to the Late Ordovician–Early Silurian opening of the PalaeoTethys ocean and to the subduction of ProtoTethys and Rheic oceans. The Hun superterrane (representing the northern margin of the PalaeoTethys ocean) was subsequently dismembered by its col-

lision with Baltica-Avalonia in Late Devonian–Early Carboniferous times, and its different parts were stacked in front of each other to form the European Variscan orogen (Fig. 9b). The collisional events were complex and produced a duplication of different parts of the Hun superterrane (see Fig. 9a). Soon after the docking of the larger part of the Hun superterrane, the PalaeoTethys started subducting northward under the southern edge of the Hun terranes. The increasing slab roll back of the PalaeoTethys resulted in the collapse of the Variscan orogen and the opening of features characterized by large amounts of calc-alkaline volcanism in the Late Carboniferous grading to more alkaline volcanism in the Early Permian (see STAMPFLI, 1996, for a review).

The pre-Alpine events recorded in the Briançonnais are consistent with this model and the Briançonnais zone is considered to be a result of the juxtaposition of Variscan terranes representing the frontal part of a segment of the Hun superterrane. The Gondwanan, Pan-African origin of the Western Alpine basements is confirmed by some Proterozoic to Early Palaeozoic ages recorded in nearly all of them (BUSSY et al., 1996b; GUILLOT et al., 1991). The onset of the PalaeoTethys rifting in the context of a back-arc is recorded by the presence of either alkaline or calc-alkaline intrusions and volcanics of Ordovician age. The subduction of the Rheic sea-floor ac-

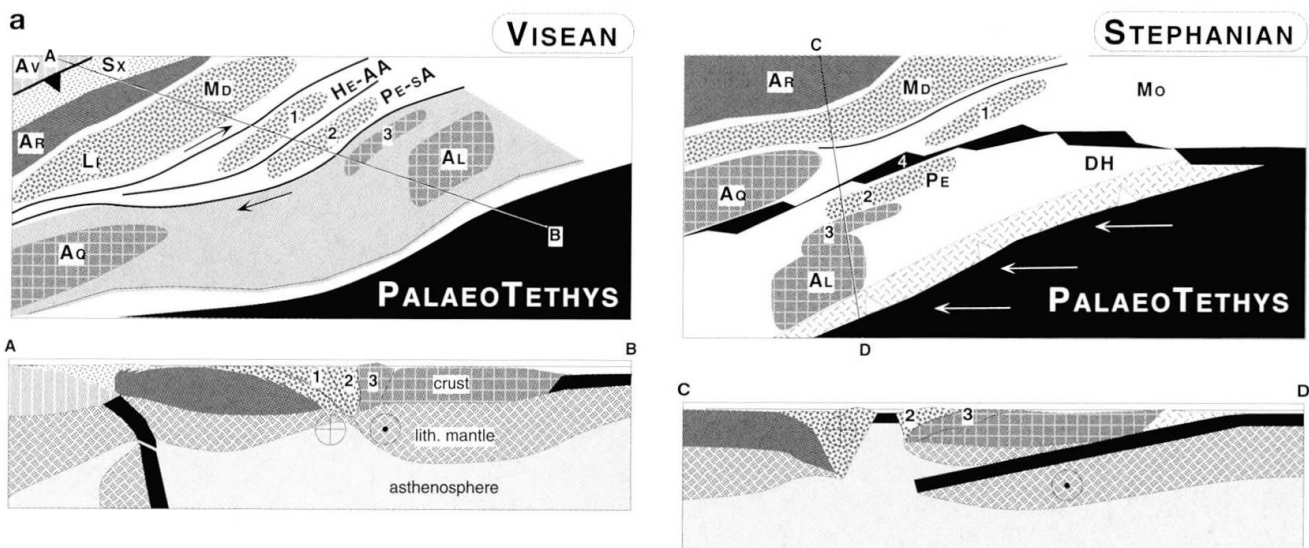
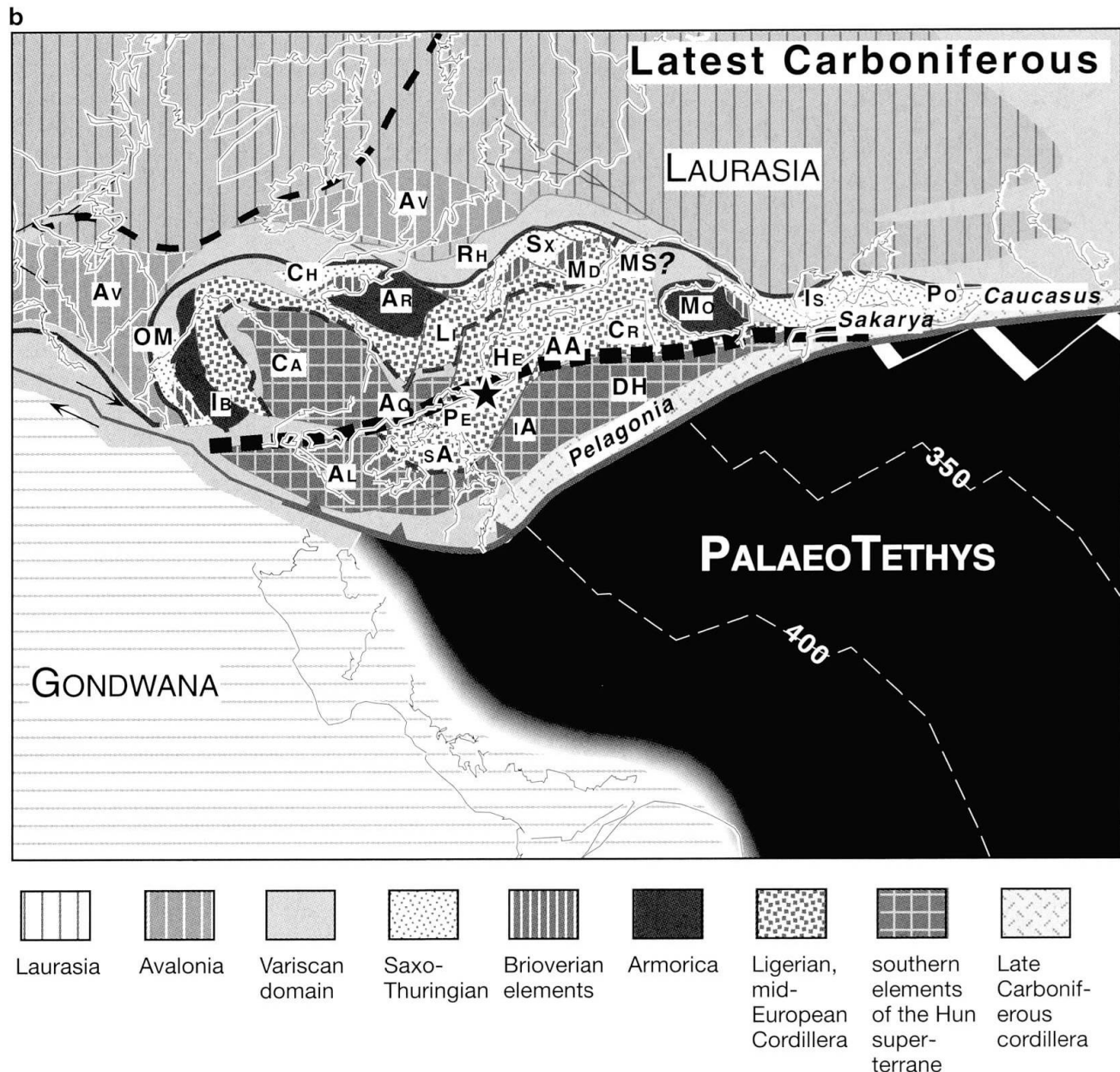


Fig. 9 (a): Schematic evolution of the Variscan orogen in Visean and Stephanian times. Large scale right lateral strike slip movements duplicated the former ribbon like Hun Gondwana terranes (see legend in Fig. 9b) following its collision with Avalonia (Av) and Baltica. The Hun Cordillera terranes (see legend in Fig. 9b) located on the northern active margin of the Hun superterrane are also duplicated and affected by extension. The Helvetic (1) and external Briançonnais (2) domains belonged to these cordilleras, the internal Briançonnais domain (3) corresponded to the former northern border of the intra-Alpine domain. (1) and (2) were separated by a pull-apart rift system in Late Carboniferous, represented in the Briançonnais area by the Zone Houillère (4).

companying the Hun Superterrane accretion is recorded by the presence of eclogites whose metamorphism is dated as Early Silurian (PAQUETTE et al., 1989). The initial phase of Variscan collision in the Briançonnais domain is recorded through the Late Devonian metamorphism of some gneiss (e.g. Sapey gneiss, older than 360 Ma, BERTRAND et al., 1998), this complex collisional

event lasted until the mid-Carboniferous with a peak metamorphism around 330 Ma (latest Visean). The major strike-slip motion due to back-arc spreading that affects the former cordillera is recorded by intrusions and extrusions of Late Carboniferous calc-alkaline to alkaline material in the zone Houillère (BERTRAND et al., 1998; CORTESOGNO et al., 1992; CORTESOGNO



(b) Latest Carboniferous reconstruction of the western Tethyan realm (modified after STAMPFLI et al., in press) showing the distribution of the different elements derived from the Hun superterrane. Large parts of the Hun superterrane have been displaced laterally along a right lateral pull-apart system (large black dashed line). The star indicates the area studied in this paper.

**Hun Cordillera terranes:** Early Palaeozoic active margin of the Hun composite terrane from west to east: OM, Ossava Morena; CH, Channel terrane; SX, Saxo-Thuringian; Is, Istanbul; Po, Pontides; LI, Ligerian; MD, Moldanubian; MS, Moravo-Silesicum; HE, Helvetic; SA, south-Alpine; PE, Penninic; AA, Austroalpine; CR, Carpathian.

**Hun Gondwana terranes:** blocks which formed the northern margin of PalaeoTethys, from west to east: IB, Iberic; AR, Armorica; MO, Moesia; CT, Cantabrian; AQ, Aquitaine; AL, Alboran; IA, intra-Alpine (Adria, Carnic, Austro-Carpathian); DH, Dinaric-Hellenic.

et al., 1993), and by P-T-t paths recorded for units such as the Mont-Mort, that are characteristic of a rapid decompression in an extensional regime.

A former common history of the Helvetic (1 in Fig. 9a) and outer Briançonnais (Ruitor, Pontis) elements (2 in Fig. 9a) is likely as discussed above. Both domains were part of the cordillera bordering the Hun superterrane to the north. These cordilleras are thought to have evolved from the accretion of material off-scraped from the subducting ProtoTethys and Rheic oceans and the subsequent metamorphism of this material by arc-related intrusions. The less metamorphic domain in the inner Briançonnais domain (Siviez, Mont Fort, 3 in Fig. 9a) is interpreted as a potential back-stop of the accretionary prism, therefore it represents the uplifted Panafrican basement of the Intra-Alpine or Noric terrane (VON RAUMER AND NEUBAUER, 1993). The zone Houillère appeared between the Helvetic and Briançonnais domain in Late Carboniferous when both domains were separated. It is through the rifting events affecting the Alpine and Iberic areas in Jurassic and Cretaceous times and the subsequent closure of the Alpine Tethys and Valais domain (STAMPFLI and MARCHANT, 1997; STAMPFLI et al., 1998) that the Briançonnais was brought back in front of the Helvetic margin as an Alpine exotic terrane (STAMPFLI, 1993). During the Alpine orogenic event a thin basement sliver and its cover (the Préalpes) was detached from its substratum and obducted onto the European margin. This obduction certainly explains the lack of an Alpine metamorphic overprint for part of the Briançonnais basement as recorded in the Mont-Mort area.

## 7. Conclusions

An extremely weak Alpine overprint in the Mont-Mort metapelites preserved magnificent mineral assemblages indicative of amphibolite facies metamorphism. These assemblages are consistent with a nearly isothermal decompressive P-T-t path during the Variscan orogeny. Geothermobarometry indicates P-T conditions of 600 °C / 5–8 kbar to 550 °C / 2 kbar, which are comparable to estimates by VON RAUMER (1983) for the Emosson metapelites (Helvetic basement). A very high geothermal gradient (around 80 °C/km) was present at the end of the decompression. This thermal evolution is ascribed to the post-collisional extension of a thickened crust.

Andalusite-bearing veins could be evidence for a high T-P gradient at the end of the Variscan metamorphism. Corundum and diaspore crystal-

lized through hydration processes during retrogression.

The peak of metamorphism has been dated at 330 Ma, whereas closure of the Ar muscovite system occurred at 290–310 Ma. However, it is not yet clear if the proposed path was continuous or not. There is no geochronological evidence for any pre-Variscan metamorphic basement as indicated on the pre-Alpine metamorphic map of the Alps (DESMONS et al., 1999).

The reason that the Alpine overprint was so weak in the Mont-Mort unit can be explained by the obduction of the external Briançonnais terrane during Alpine tectonic events, preserving the Variscan assemblages in the frontal part of this terrane.

From a Palaeozoic point of view, the Briançonnais zone is regarded as a juxtaposition of Variscan terranes representing parts of the Hun superterrane that was accreted from Late-Devonian to Middle-Carboniferous times. The P-T-t path indicates a rapid decompression in an extensional regime associated with the collapse and duplication of the Variscan Cordillera. This model allows the passage from a M-P / H-T regime (collision) to a L-P / H-T one with a high geothermal gradient (extensional regime associated with the opening of the zone Houillère) as recorded within the Mont-Mort metapelites to be explained.

## Acknowledgements

We thank Marcel Burri, Jürgen von Raumer and Yves Gouffon for field work assistance and fruitful and very pleasant discussions, Mike Cosca and Greg Roselle for English correction and helpful and constructive comments, Raymond Ansermoz and Laurent Nicod for preparation of thin and polished sections and several anonymous colleagues who improved earlier and the present versions of the manuscript. M. Engi and an anonymous reviewer greatly helped to clarify the paper. FB is indebted to T. Krogh and D. Davis, Royal Ontario Museum, for access to their geochronology laboratory, and for technical and scientific support. This work was, in part, supported by the Swiss National Science Foundation (FNRS grants, project No. 2100-049410.96 and 21-45650). A special thank you from DG to "Felice del Gd-St-Bernard", owner of the "Bar du Lac".

## References

- BAUDIN, T. (1987): Etude géologique du massif du Ruitor (Alpes franco-italiennes): évolution structurale d'un socle briançonnais. Thèse Univ. Grenoble, 259 pp.
- BERTRAND, J.M., GUILLOT, F., LETERRIER, J., PERRUCHOT, M.D., AILLIÈRES, L. and MACAUDIÈRE, J. (1998): Granitoïdes de la zone Houillère briançonnais.

naisse en Savoie et en Val d'Aoste (Alpes occidentales): géologie et géochronologie U/Pb sur zircon. *Geodinamica Acta*, 11, 33–49.

BEARTH, P. (1978): Feuille St. Niklaus et sa notice explicative. *Atlas géologique de la Suisse*. 1 : 25'000. Kümmerly et Frey, Berne.

BOCQUET [DESMONS], J. (1974): Etudes minéralogiques et pétrographiques sur les métamorphismes d'âge alpin dans les Alpes françaises. Thèse Grenoble, 489 pp.

BOCQUET [DESMONS], J., DELALOYE, M., HUNZIKER, J.C. and KRUMMENACHER, D. (1974): K-Ar and Rb-Sr dating of blue amphiboles, micas and associated minerals from the Western Alps. *Contrib. Mineral. Petrol.*, 47, 7–26.

BRUGGER, J. (1994): Les veines à andalousite du Pischa-horn (Grisons, Suisse). *Schweiz. Mineral. Petrogr. Mitt.*, 74, 191–202.

BURRI, M. (1983): Description géologique du front du Saint-Bernard dans les vallées de Bagnes et d'Entremont (Valais). *Bull. Lab. Géol. Univ. Lausanne* n° 270, 88 pp.

BUSSY, F. and VON RAUMER, J.F. (1993): U-Pb dating of Palaeozoic event in the Mont-Blanc crystalline massif, Western Alps. *Terra Nova*, 1995, vol. 5, suppl. 1, 187–188.

BUSSY, F., SARTORI, M. and THÉLIN, P. (1996a): U-Pb zircon dating in the middle Penninic basement of the Western Alps (Valais, Switzerland). *Schweiz. Mineral. Petrogr. Mitt.*, 76, 81–84.

BUSSY, F., DERRON, M.H., JACQUOD, J., SARTORI, M. and THÉLIN, P. (1996b): The 500 Ma old Thyon meta-granite. New A-type granite occurrence in the Penninic realm (Western Alps, Wallis, Switzerland). *Eur. J. Mineral.*, 8, 565–575.

BUSSY, F. and HERNANDEZ, J. (1997): Short-lived bimodal magmatism at 307 Ma in the Mont-Blanc/Aiguilles-Rouges area: A combination of decompression melting, basaltic underplating and crustal fracturing. Abstract of 3rd workshop on Alpine Geological Studies, Oropa-Biella.

CABY, R. (1996): Low-angle extrusion of high-pressure rocks and the balance between outward and inward displacements of Middle Penninic units in the western Alps. *Eclogae geol. Helv.* 89/1, 229–267.

CESARE, B. (1992): Metamorfismo di contatto di rocce pelitiche nell'aureola di Vedrette di Ries (Alpi Orientali, Italia). Thesis, Università di Padova, Italy.

CHESSEX, R. (1995): Tectonomagmatic setting of the Mont Fort nappe basement, Penninic domain, western Alps, Switzerland. In: PISKIN, O., ERGUN, M., SAVASCIN, M.Y. and TARCAN, G. (eds): Intern. Earth Sciences colloquium on the Aegean region. Proceedings, I, 19–35.

CORTESOGNO, L., DALLAGIOVANNA, G., GAGGERO, L. and VANOSSI, M. (1992): Late Variscan intermediate volcanism in the Ligurian Alps. In: CARMIGNANI, L. and SASSI, F.P. (eds): Contribution to the geology of Italy. IGCP 276 Newsletters 5, Siena, 241–262.

CORTESOGNO, L., DALLAGIOVANNA, G., GAGGERO, L. and VANOSSI, M. (1993): Elements of the Palaeozoic history of the Ligurian Alps. In: VON RAUMER, J.F. and NEUBAUER, F. (eds): Pre-Mesozoic geology of the Alps. Springer Verlag, Berlin Heidelberg, 257–277.

COSCA, M.A., MEZGER, K. and ESSENE, E. (1998): The Baltica-Laurentia Connection: Sveconorwegian (Grenvillian) metamorphism, cooling and unroofing in the Bamble Sector, Norway. *J. Geol.*, 106, 539–552.

DESMONS, J. (1992): The Briançon basement (Pennine Western Alps): mineral composition and polymeta-morphic evolution. *Schweiz. Mineral. Petrogr. Mitt.*, 72, 37–55.

DESMONS, J., LADURON, D. and DE BÉTHUNE, P. (1977): Grenats zonés de la nappe du Grand Saint Bernard et de la zone piémontaise (Alpes occidentales). *Mém. Inst. Géol. Univ. Louvain*, 29, 327–347.

DESMONS, J., COMPAGNONI, R., CORTESOGNO, L., FREY, M. and GAGGERO, L. (1999): Pre-Alpine metamorphism of the Internal zones of the Western Alps. *Schweiz. Mineral. Petrogr. Mitt.*, 79, 23–39.

DÉTRAZ, G. and LOUBAT, H. (1984): Faciès à disthène, staurotide et grenat dans un micaschiste appartenant à l'unité des "gneiss du Sapey" (Vanoise, Alpes françaises). *Géologie Alpine*, 60, 5–12.

EISELE, J., GEIGER, S. and RAHN, M. (1997): Chemical characterization of metabasites from the Turtmann-valley (Valais, Switzerland): implication for their protoliths and geotectonic origin. *Schweiz. Mineral. Petrogr. Mitt.*, 77, 403–418.

ESCHER, A., MASSON, H. and STECK, A. (1993): Nappe geometry in the Western Swiss Alps. *J. Struct. Geol.*, 15, 501–509.

GHENT, E.D. and STOUT, M.Z. (1981): Geobarometry and geothermometry of plagioclase-biotite-garnet-muscovite assemblages. *Contrib. Mineral. Petrol.*, 76, 92–97.

GIORGIS, D. (1997): Etude du métamorphisme de la partie septentrionale de l'ensemble du Mont Mort, Nappe des Pontis, Col du Grd St-Bernard, Valais. Travail de diplôme, Université de Lausanne, unpubl.

GOUFFON, Y. (1993): Géologie de la "nappe" du Grand St-Bernard entre la Doire Baltée et la frontière suisse (Vallée d'Aoste, Italie). *Mém. Géol. Lausanne*, 12, 1–147.

GOUFFON, Y. and BURRI, M. (1997): Les nappes des Pontis, de Siviez Mischabel et du Mont Fort dans les vallées de Bagnes, d'Entremont (Valais, Suisse) et d'Aoste (Italie). *Eclogae geol. Helv.*, 90, 29–41.

GUIDOTTI, C. (1984): Micas in metamorphic rocks. In: BAILEY, S.W. (ed.): *Micas. Reviews in Mineralogy*, 13, MSA. Chap. 10, 357–467.

GUILLOT, F., LIÉGEOIS, J.P. and FABRE, J. (1991): Des granophyres du Cambrien terminal dans le Mont Pourri (Vanoise, zone brançonnaise): première datation U-Pb sur zircon d'un socle des zones internes des Alpes françaises. *C. R. Acad. Sci. Paris*, 313, II, 239–244.

GUILLOT, F., DESMONS, J. and PLOQUIN, A. (1993): Lithostratigraphy and geochemical composition of the Mont Pourri volcanic basement, Middle Penninic, W-Alpine zone, France. *Schweiz. Mineral. Petrogr. Mitt.*, 73, 319–334.

HEDIGER, R. (1979): Géologie et pétrographie du Col du Grand St-Bernard. Travail de diplôme, Université de Lausanne, unpubl.

HEMLEY, J.J., MONTOYA, J.W., MARINENKO, J.W. and LUCE, R.W. (1980): Equilibria in the system  $\text{Al}_2\text{O}_3$ – $\text{SiO}_2$ – $\text{H}_2\text{O}$  and some general implications for alteration/mineralization processes. *Econ. Geol.*, 75, 210–228.

HODGES, K.V. and SPEAR, F.S. (1982): Geothermometry, geobarometry and the  $\text{Al}_2\text{SiO}_5$  triple point at Mt. Moosilauke, New Hampshire. *Amer. Mineral.*, 67, 1118–1134.

HOLDAWAY, M.J. (1971): Stability of andalusite and the aluminum silicate phase diagram. *Amer. J. Science*, 271, 97–131.

HOSCHEK, G. (1969): The stability of staurolite and chloritoid and their significance in metamorphism of pelitic rocks. *Contrib. Mineral. Petrol.*, 22, 208–232.

HUBER, R.K. (1999): Tectonometamorphic evolution of

the Eastern Pennine Alps during Tertiary continental collision: Structural and petrological relationships between Suretta, Tambo, Chiavenna and Gruf units (Switzerland/Italy). Thèse Univ. Neuchâtel, 311 pp.

HUNZIKER, J.C., DESMONS, J. and HURFORD, A.J. (1992): Thirty-two years of geochronological work in the Central and Western Alps: a review on seven maps. *Mém. Géol. Lausanne*, 13, 1–59.

KIRSCHNER, D.L., COSCA, M.A., MASSON, H., HUNZIKER, J.C. (1996): Staircase  $^{40}\text{Ar}/^{39}\text{Ar}$  spectra of fine-grained white mica: Timing and duration of deformation and empirical constraints on argon diffusion. *Geology*, 24, 747–750.

KRAMAR, N., COSCA, M.A., HUNZIKER, J.C. (in prep.): Distribution and significance of radiogenic argon in deformed muscovite: evidence from in-situ UV-laser ablation  $^{40}\text{Ar}/^{39}\text{Ar}$  geochronology.

LIÉGEOIS, J.P. and DUCHESNE, J.C. (1981): The Lac Cornu retrograded eclogites (Aiguilles Rouges Massif, Western Alps, France): evidence of crustal origin metasomatic alteration. *Lithos*, 14, 35–48.

MASON, R. (1978): Petrology of metamorphic rocks. George Allen and Unwin Ltd., 254 pp.

MARKLEY, M., COSCA, M., CABY, R., HUNZIKER, J.C. and SARTORI, M. (1998): Alpine deformation and  $^{40}\text{Ar}/^{39}\text{Ar}$  geochronology of synkinematic white micas in the Siviez-Mischabel Nappe, western Penninic Alps, Switzerland. *Tectonics*, 17, 407–425.

MEZGER, K., ESSENE, E. and HALLYDAY, A.N. (1992): Closure temperature for the Sm/Nd System in metamorphic garnets. *Earth Planet. Sci. Lett.*, 88, 82–92.

MONIÉ, P. (1990): Preservation of Hercynian Ar/Ar ages through high-pressure low-temperature Alpine metamorphism in the Western Alps. *Eur. J. Mineral.*, 2, 343–361.

OULIANOFF, N. and TRÜMPY, R. (1958): Feuille Grand Saint-Bernard et sa notice explicative. Atlas géologique suisse. 1:25'000. Kümmerly et Frey, Berne.

PAQUETTE, J.L., MÉNOT, R.P. and PEUCAT, J.J. (1989): REE, Sm–Nd and U–Pb zircon study of eclogites from the Alpine External massifs (Western Alps): evidence for crustal contamination. *Earth Planet. Sci. Lett.*, 96, 181–198.

PERCHUK, L.L. (1991): Progress in metamorphic and magmatic petrology. Cambridge University Press, 503 pp.

VON RAUMER, J.F. (1983): Die Metapelite von Emosson (Aiguilles Rouges Massiv) als Beispiel spätkalédonisch-frühvariszischer Metamorphose im Alt-kristallin des helvetisches Bereichs. *Schweiz. Mineral. Petrogr. Mitt.*, 63, 421–455.

VON RAUMER, J.F. and NEUBAUER, F. (1993): Late Precambrian and Palaeozoic Evolution of the Alpine Basement – An Overview. In: VON RAUMER, J.F. and NEUBAUER, F. (eds): Pre-Mesozoic geology in the Alps. Springer Verlag, Berlin Heidelberg, 625–639.

ROSE, R.L. (1957): Andalusite and corundum-bearing pegmatites in Yosemitic National Park, California. *Amer. Mineral.* 42, 635–647.

SARTORI, M., BUGNON, P.C., FREY, M., GANGUIN, J., MASSON, H., STECK, A. and THÉLIN, P. (1989): Compte-rendu de l'excursion commune de la SSMP et de la SGS le long du profil Rawil-Zermatt, 9/10/11 octobre 1988. *Schweiz. Mineral. Petrogr. Mitt.*, 69, 261–281.

SHULTERS, J.C. and BOHLEN, S.R. (1989): The stability of hercynite and hercynite gahnite spinels in corundum or quartz-bearing assemblages. *J. Petrol.*, 30, 1017–1031.

SOOM, M.A. (1990): Abkühlungs- und Hebungsgeschichte der Externmassive und der penninischen Decken beidseits der Simplon–Rhone-Linie seit dem Oligozän. Spaltspurdatierungen an Apatit/Zirkon und K-Ar-Datierungen an Biotit/Muskowit (westliche Zentralalpen). *Diss. Univ. Bern*, 64 pp.

SPAENHAUER, A. (1933): Die Andalusit- und Disthenvorkommen der Silvretta. *Schweiz. Mineral. Petrogr. Mitt.*, 13, 323–346.

SPEAR, F.S. (1993): Metamorphic phase equilibria and pressure-temperature-time paths. *Monograph of Mineral. Soc. Am.*, Washington, D.C., 799 pp.

SPEAR, F.S. and CHENEY, J.T. (1989): A petrogenetic grid for pelitic schists in the system  $\text{SiO}_2\text{--Al}_2\text{O}_3\text{--FeO--MgO--K}_2\text{O--H}_2\text{O}$ . *Contrib. Mineral. Petrol.*, 101, 149–164.

STAMPFLI, G.M. (1993): Le Briançonnais, terrain exotique dans les Alpes? *Eclogae geol. Helv.*, 86, 1–45.

STAMPFLI, G.M. (1996): The Intra-Alpine terrain: a Paleotethyan remnant in the Alpine Variscides. *Eclogae geol. Helv.* 89/1, 13–42.

STAMPFLI, G.M. and MARCHANT, R.H. (1997): Geodynamic evolution of the Tethyan margins of the Western Alps. In: PFIFFNER, O.A., LEHNER, P., HEITZMANN, P.Z., MUELLER, S. and STECK, A. (eds): Deep structure of the Swiss Alps – Results from NRP 20. Birkhäuser AG, Basel, 223–239.

STAMPFLI, G.M., MOSAR, J., MARCHANT, R., MARQUER, D., BAUDIN, T. and BOREL, G. (1998): Subduction and obduction processes in the western Alps. In: VAUCHEZ, A. and MEISSNER, R. (eds): Continents and their mantle roots. *Tectonophysics*, 296, 159–204.

STAMPFLI, G.M., MOSAR, J., FAVRE, P., PILLEVUIT, A. and VANNAY, J.-C. (in press): Late Palaeozoic to Mesozoic evolution of the western Tethyan realm: the Neotethys/East-Mediterranean connection. In: CAVAZZA, W., ROBERTSON, A.H.F.R. and ZIEGLER, P.A. (eds): Peritethyan rift/wrench basins and passive margins, IGCP 369, *Bull. Museum Nat. Hist. Nat.*, Paris.

THÉLIN, P. (1992): Les métapélites du Mont-Mort: une fenêtre métamorphique (Nappe des Pontis, Zone du Ruitor, Valais). *Bull. Lab. Géol. Univ. Lausanne*, n° 315, 97–116.

THÉLIN, P., SARTORI, M., LENGELE, R., SCHEARER, J.P. (1990): Eclogites of Palaeozoic or early Alpine age in the basement of the Penninic Siviez-Mischabel nappe, Wallis, Switzerland. *Lithos*, 25, 71–88.

THÉLIN, P., SARTORI, M., BURRI, M., GOUFFON, Y. and CHESSEX, R. (1993): The pre-Alpine basement of the Briançonnais (Wallis, Switzerland). In: VON RAUMER, J.F. and NEUBAUER, F. (eds): Pre-Mesozoic geology in the Alps, Springer Verlag, Berlin Heidelberg, 297–315.

THÉLIN, P., GOUFFON, Y. and ALLIMANN, M. (1994): Caractéristiques et métamorphisme des phyllosilicates dans la partie occidentale de la "super" nappe du Grand St-Bernard (Val d'Aoste et Valais). *Bull. Lab. Géol. Univ. Lausanne*, n° 327, 93–145.

VANNAY, J.C. and GRASEMAN, B. (1998): Inverted metamorphism in the High Himalaya of Himachal Pradesh (NW India): phase equilibria versus thermometry. *Schweiz. Mineral. Petrogr. Mitt.* 78, 107–132.

YARDLEY, B.W.D. (1989): An introduction to metamorphic petrology. Longman Singapore Publishers (Pte) Ltd., 248 pp.